

MISO PRECODING FOR TEMPORAL AND SPATIAL FOCUSING

Robert C. Daniels and Robert W. Heath, Jr.

Wireless Networking and Communications Group
University of Texas at Austin
{rdaniels, rheath}@ece.utexas.edu

ABSTRACT

Time reversal precoding accomplishes matched-filtering of the channel in wireless communication systems by precoding before every transmit antenna with the time reversed complex conjugate of the wireless channel impulse response. While time reversal maximizes the received signal energy at a single time instant (as with matched filtering) it does not eliminate intersymbol interference. This is equivalent to saying that the combined precoder/channel response has significant temporal sidelobes and thus, not sufficiently temporally focused. We propose a method of multiple-input-single-output (MISO) precoding for lowering sidelobe levels to improve temporal focusing. Through simulations, we analyze and show improved spatial focusing properties of the developed method in correlated and uncorrelated frequency selective channels. Although equalizer design is absent in this paper, we include equalizer length into the optimization, using a methodology similar to channel shortening, such that flexible communication system solutions easily follow.

1. INTRODUCTION

Time reversal pre-filtering was introduced in [1] for ultrasonic applications. Time reversal is accomplished by pre-filtering with the time reversed, complex conjugate of the channel between each transmit antenna and the receiver. As is well known in both the radar and communications literature, this is equivalent to using the channel as a matched filter. The matched filter maximizes the signal energy at a single point in time [11]. In addition, it was shown that with this time reversal pre-filtering method the effective pre-filter/channel impulse response is constrained both in time and in space. Recently, time reversal pre-filtering was extended to wireless communications. Preliminary work has

shown that time reversal wireless communications also displays temporal and spatial focusing of the effective channel response [4] [5] [6].

Both temporal and spatial focusing are desired in wireless communications systems for a variety of reasons. Temporal focusing relates to a measure of the received signal energy in some window of time. Wireless channels, in general, tend to spread transmitted signals over time [10] causing intersymbol interference (ISI). Time reversal compresses the transmitted signal such that the spreading effect of the wireless channel is not as dramatic. Spatial focusing, on the other hand, relates to the received signal energy for receivers at different locations in space. Since time reversal pre-filters are a function of the channel for some targeted receiver, time reversal spatially focuses signals towards that targeted receiver. Receivers outside of the target will, in general, receive much degraded signal quality.

In this paper, we consider a sampled multiple transmit antenna pre-filtered wireless communications system which we term a MISO precoding system. We show that one can improve on time reversal by optimally focusing the effective channel impulse response, and at the same time maintain the important property of spatial focusing. Pre-filtering methods that optimize error rate performance have already been studied in detail [13] [15]. Since temporal focusing quality relates to error rate performance, we cannot hold our precoder's value on this alone. There are two qualities of the precoding design proposed in this paper that separate it from previous work:

1. We allow for an adaptable number of desired taps in the equalizer. Similar to channel shortening [3], we "focus" as much energy into the desired taps as possible. Indirectly, the proposed precoder includes equalizer design.
2. Few have investigated pre-filtering methods outside of time reversal in terms spatial focusing and for frequency selective channels. [14] implemented zero forcing combined with time reversal precoding, but this was not derived from a single optimal precoding method as considered in this paper, limiting the performance, flexibility and universal application.

Robert C. Daniels is supported by the Microelectronics and Computer Development Fellowship and the Basdall Gardner Memorial Graduate MCD Fellowship in Engineering at the University of Texas at Austin.

Robert W. Heath, Jr. is supported in part by the Office of Naval Research under grant number N00014-05-1-0169.

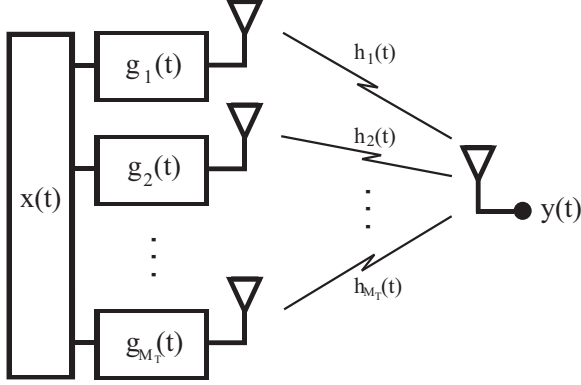


Figure 1: Model of the MISO system for time-reversal wireless

The organization of the paper will be as follows. In Section 2 we detail the system description for both time reversal and general MISO precoding. In Section 3 we give the focusing (temporal and spatial) definitions to be used throughout the paper. Section 4 derives the temporal focusing optimal precoder. In Section 5 we investigate the performance of this precoder compared to time reversal through simulations. Throughout this paper we use boldface lower case letters, \mathbf{a} , to denote vectors, boldface uppercase letters, \mathbf{A} , to denote matrices, \mathbf{I} is the identity matrix, $\mathbf{A}_{i \rightarrow j}$ is the matrix composed of rows i through j of \mathbf{A} , $*$ for complex-conjugate, $(\bullet)^T$ for matrix transpose, and $(\bullet)^H$ for matrix complex-conjugate transpose. $\Re\{\bullet\}$ and $\Im\{\bullet\}$ indicates the real and imaginary part respectively of the quantities inside the brackets.

2. SYSTEM DESCRIPTION

2.1. Time Reversal

The wireless communications extension of the time reversal work in acoustics uses multiple (M_T to be precise) transmit antennas in place of the multiple channel sounders [1] [6]. A graphical description of this continuous-time time reversal wireless system can be seen in Figure 1. In this figure, $x(t)$ refers to the transmitted signal, $g_i(t)$ is the pre-filter impulse response for antenna i , $h_i(t)$ is the channel impulse response between transmit antenna i and the receiver, and $y(t)$ is the received signal. In a pure time-reversal system $g_i(t) = h_i^*(-t)$. In this paper we will consider more general filter designs.

Assuming a linear time-invariant system description

$$y(t) = x(t) * \left(\sum_{i=1}^{M_T} (g_i * h_i)(t) \right)$$

where $*$ denotes continuous-time convolution. Because most modern communication systems are digital, it is important for us to consider sampling of the pre-filtered system. We shall consider the quantity $y[n] = y(nT_s)$ which, as we

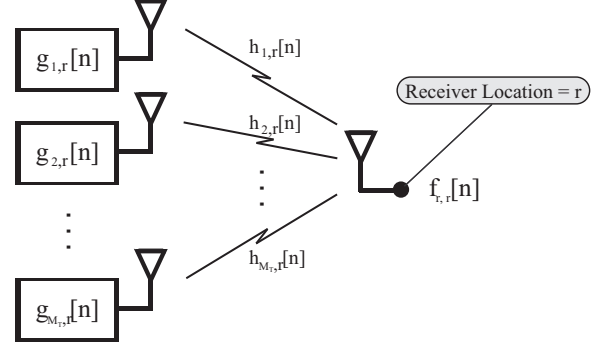


Figure 2: Model of the sampled MISO system under analysis for precoder optimization

shall see in the next section, represents the sampled output signal.

2.2. MISO Precoding

Consider the multiple-input single-output (MISO) discrete-time system with precoding at each antenna as pictured in Figure 2. This discrete-time system description is valid for inputs sampled above the Nyquist frequency. Let $h_{i,r'}[n]$ denote the length ν discrete-time impulse response between the i^{th} transmitter and the intended receiver at location r' . The location vector \mathbf{r} is typically defined in the three dimensional space, but is sometimes assumed to be two or one dimensional if one or two of the dimensions, respectively, remain consistent throughout. Let $g_{i,r}[n]$ denote the length L precoding filter whose design we will optimize for some specific location \mathbf{r} . It is useful to note that in a general time reversal MISO system $g_{i,r}[n] \triangleq \alpha_i h_{i,r}^*[\nu - n]$ for some constant α_i which is used in several schemes to enforce some transmit power constraint. The discrete-time effective precoder/channel impulse response observed at the receiver location r' with precoders designed for location \mathbf{r} is

$$f_{\mathbf{r},\mathbf{r}'}[n] = \sum_{i=1}^{M_T} g_{i,\mathbf{r}}[n] * h_{i,\mathbf{r}'}[n] \quad (1)$$

where $*$ represents discrete-time convolution. Note that in time-reversal systems $f_{\mathbf{r},\mathbf{r}'}[n]$ for $n \neq \nu$ are the temporal sidelobes which are, in general, nonzero.

We find it convenient to formulate this model in matrix notation by defining $\mathbf{g}_{i,\mathbf{r}} \triangleq [g_{i,\mathbf{r}}[0] g_{i,\mathbf{r}}[1] \cdots g_{i,\mathbf{r}}[L-1]]^T$, $\mathbf{f}_{\mathbf{r},\mathbf{r}'} \triangleq [f_{\mathbf{r},\mathbf{r}'}[0] f_{\mathbf{r},\mathbf{r}'}[1] \cdots f_{\mathbf{r},\mathbf{r}'}[L+\nu-2]]^T$, $\mathbf{H}_{i,\mathbf{r}'}$ is the toeplitz matrix with first column $[h_{i,\mathbf{r}'}[0] \cdots h_{i,\mathbf{r}'}[\nu-1] \ 0 \ \dots \ 0]^T$ and first row $[h_{i,\mathbf{r}'}[0], 0, \dots, 0]$ such that $\mathbf{f}_{\mathbf{r},\mathbf{r}'} = \sum_{i=1}^{M_T} \mathbf{H}_{i,\mathbf{r}'} \mathbf{g}_{i,\mathbf{r}}$ is another description of the effective channel response. Furthermore, we define $\mathbf{H}_{\mathbf{r}'} \triangleq [\mathbf{H}_{1,\mathbf{r}'} \mathbf{H}_{2,\mathbf{r}'} \cdots \mathbf{H}_{M_T,\mathbf{r}'}]$, $\mathbf{g}_{\mathbf{r}} \triangleq [\mathbf{g}_{1,\mathbf{r}}^T \mathbf{g}_{2,\mathbf{r}}^T \cdots \mathbf{g}_{M_T,\mathbf{r}}^T]^T$ giving the effective response matrix equation

$$\mathbf{f}_{\mathbf{r},\mathbf{r}'} = \mathbf{H}_{\mathbf{r}'} \mathbf{g}_{\mathbf{r}}. \quad (2)$$

3. FOCUSING DEFINITIONS

3.1. Temporal Focusing

Time reversal systems have been shown to exhibit temporal focusing in the effective pre-filter/channel impulse response [5]. This implies that the response is tightly constrained in time. Ideally the system's effective response is a simple impulse (Dirac delta function in continuous-time and Kronecker delta function in discrete-time). That is, time reversal *focuses* the system response such that most of the response energy is isolated in a small window of time.

Past work has characterized temporal focusing using the RMS delay spread calculation for wireless communication channels [4]. The RMS delay spread of the effective response is given by

$$\tau_{RMS} = \sqrt{\frac{\int_{-\infty}^{\infty} (\tau - \bar{\tau})^2 \mathbb{E}_h \left[\left| \left(\sum_{i=1}^{M_T} g_i \star h_i \right) (\tau) \right|^2 \right] d\tau}{\int_{-\infty}^{\infty} \mathbb{E}_h \left[\left| \left(\sum_{i=1}^{M_T} g_i \star h_i \right) (\tau) \right|^2 \right] d\tau}}$$

where \mathbb{E}_h denotes mathematical expectation over all channel realizations and

$$\bar{\tau} = \frac{\int_{-\infty}^{\infty} \tau \mathbb{E}_h \left[\left| \left(\sum_{i=1}^{M_T} g_i \star h_i \right) (\tau) \right|^2 \right] d\tau}{\int_{-\infty}^{\infty} \mathbb{E}_h \left[\left| \left(\sum_{i=1}^{M_T} g_i \star h_i \right) (\tau) \right|^2 \right] d\tau}$$

for the continuous-time system model. Using this RMS delay spread metric a temporally focused system would have a small RMS delay spread. It is well known that delay spread relates to the amount of intersymbol interference [11]. Thus temporal focusing is desired in communication systems with high delay spread channels since it reduces the intersymbol interference. In this paper we will consider an alternate, but similar measure of temporal focusing for the discrete-time model. Before we define this metric, we first define some response dependent parameters.

In this paper we develop a precoder that maximizes the energy in K taps of the effective discrete-time impulse response. Physically this means that we will need at least a K tap equalizer at the receiver to combine transmitted symbols. This methodology is very similar to the construction of optimal channel shortening sequences discussed in [3]. The energy in the desired portion of the response at receiver location \mathbf{r}' with precoders designed for location \mathbf{r} is given by

$$DES_{\mathbf{r},\mathbf{r}'}[n] \triangleq \sum_{l=\Delta}^{\Delta+K-1} f_{\mathbf{r},\mathbf{r}'}[n] \delta_k[n-l] \quad (3)$$

where Δ is the delay of the precoder and $\delta_k[n]$ refers to the Kronecker delta function. Likewise the energy of the intersymbol interference contributing portion of the response is given by

$$ISI_{\mathbf{r},\mathbf{r}'}[n] \triangleq \sum_{l=0, l \notin \{\Delta, \dots, \Delta+K-1\}}^{\nu+L-2} f_{\mathbf{r},\mathbf{r}'}[n] \delta_k[n-l]. \quad (4)$$

Finally, considering additive noise at the receiver with variance σ^2 (transmit energy normalized), we provide the measure of temporal focusing for the response at receiver location \mathbf{r}' with precoders designed for location \mathbf{r} as

$$\gamma_{TF_{\mathbf{r},\mathbf{r}'}} \triangleq \frac{\sum_n |DES_{\mathbf{r},\mathbf{r}'}[n]|^2}{\sum_n |ISI_{\mathbf{r},\mathbf{r}'}[n]|^2 + \sigma^2} \quad (5)$$

which is termed the temporal focusing ratio.

3.2. Spatial Focusing

Additionally, and perhaps more importantly, time-reversal systems display spatial focusing [6]. Spatial focusing relates the ratio of received system response energy at different points in space. Unfortunately, spatial focusing does not have a standard definition. Some have considered measuring the received average absolute signal energy at different points in space [6]. Others have looked at the peak signal energy levels in different points in space. In this paper, we consider a discrete-time spatial focusing metric that we feel best relates to communication system performance.

We assume that the desirable signal energy is forced into K taps of the discrete-time effective channel impulse response. The energy contained in these K taps will be equalized and will contribute to usable signal energy at the receiver whereas the residual energy will contribute to intersymbol interference. Therefore if we are hoping to focus the signal towards location \mathbf{r} and away from location \mathbf{r}' then we desire the signal to intersymbol interference plus noise ratio (SINR) to be large at \mathbf{r} and small at \mathbf{r}' . This leads us to our measure of spatial focusing, named the spatial focusing ratio

$$\gamma_{SF_{\mathbf{r},\mathbf{r}'}} \triangleq \frac{(\sum_n |DES_{\mathbf{r},\mathbf{r}}|^2)(\sum_n |ISI_{\mathbf{r},\mathbf{r}'}|^2 + \sigma^2)}{(\sum_n |ISI_{\mathbf{r},\mathbf{r}}|^2 + \sigma^2)(\sum_n |DES_{\mathbf{r},\mathbf{r}'}|^2)} \quad (6)$$

between the target receiver at location \mathbf{r} and the intercepting receiver at location \mathbf{r}' . Thus, high values of $\gamma_{SF_{\mathbf{r},\mathbf{r}'}}$ yield a system that is focused towards \mathbf{r} and away from \mathbf{r}' .

4. PRECODER OPTIMIZATION

We maximize the energy in the K desired taps while minimizing the energy in the remaining undesired taps of the effective channel response. Assuming additive noise at the receiver (transmitted signal energy normalized), the objective is to maximize the desired response energy to undesired response energy plus noise ratio (with precoder energy normalized). Thus,

$$\begin{aligned} \mathbf{g}_{TF_{\mathbf{r},K}} &= \arg \max_{\mathbf{g} \in \mathbb{C}^{M_T L}, \|\mathbf{g}\|^2=1} \{ \gamma_{TF_{\mathbf{r},\mathbf{r}'}} \} \\ &= \arg \max_{\|\mathbf{g}\|^2=1} \left\{ \frac{\sum_n |DES_{\mathbf{r},\mathbf{r}}[n]|^2}{\sum_n |ISI_{\mathbf{r},\mathbf{r}}[n]|^2 + \sigma^2} \right\} \quad (7) \end{aligned}$$

formulates the temporal focusing optimal precoder for receiver location \mathbf{r} . We let $\mathcal{H}_{DES,\mathbf{r}} \triangleq [\mathbf{H}_{\mathbf{r}}]_{\Delta \rightarrow (\Delta+K-1)}$ and

$$\begin{aligned}
\mathbf{A} &\triangleq \mathcal{H}_{DES,r}^H \mathcal{H}_{DES,r}. \text{ Let } \mathcal{H}_{ISI,r} \triangleq [[\mathbf{H}_r]_{1 \rightarrow (\Delta-1)} \\
&[\mathbf{H}_r]_{\Delta+K \rightarrow (L+\nu-1)}]^T \text{ and } \mathbf{B} \triangleq \mathcal{H}_{ISI,r}^H \mathcal{H}_{ISI,r} + \sigma^2 \mathbf{I}, \text{ so} \\
&\text{that equivalently} \\
\mathbf{g}_{TF,K} &= \arg \max_{\mathbf{g} \in \mathbb{C}^{M_T L}, \|\mathbf{g}\|^2=1} \left\{ \frac{\|\mathcal{H}_{DES,r} \mathbf{g}\|^2}{\|\mathcal{H}_{ISI,r} \mathbf{g}\|^2 + \sigma^2} \right\} \\
&= \arg \max_{\|\mathbf{g}\|^2=1} \left\{ \frac{\mathbf{g}^H \mathbf{A} \mathbf{g}}{\mathbf{g}^H \mathbf{B} \mathbf{g}} \right\}. \quad (8)
\end{aligned}$$

When \mathbf{A} , \mathbf{B} , and \mathbf{g} have real entries this ratio is simply the generalized Rayleigh quotient which has solution such that $\mathbf{A} \mathbf{g}_{TF,K} = \lambda \mathbf{B} \mathbf{g}_{TF,K}$ for some $\lambda \in \mathbb{R}$. Thus the generalized eigenvalue of maximum absolute value for matrices \mathbf{A} and \mathbf{B} is the solution [8]. For complex entries matrix differentiation shows that $\gamma \mathbf{g}'^T (\mathbf{B}_1 + \mathbf{B}_1^T) = \mathbf{g}'^T (\mathbf{A}_1 + \mathbf{A}_1^T)$ where γ is the maximum value taken in (7), $\mathbf{g}' = [\Re\{\mathbf{g}\}^T \Im\{\mathbf{g}\}^T]^T$, and

$$\mathbf{A}_1 \triangleq \begin{bmatrix} \Re\{\mathbf{A}\} & -\Im\{\mathbf{A}\} \\ \Im\{\mathbf{A}\} & \Re\{\mathbf{A}\} \end{bmatrix}.$$

\mathbf{B}_1 and \mathbf{B} follow the same relationship. Therefore, finding the solution for complex entries is again a generalized eigenvalue problem. Stable methods for computing generalized eigenvalues, such as the QZ method, are well known and can be referenced in [12]. Moreover, if we know that \mathbf{A} and \mathbf{B} are symmetric positive definite (as is the case in this paper) more efficient algorithms for computing generalized eigenvalues are available [12].

5. EXPERIMENTAL ANALYSIS

In this section we analyze the impact of the MISO precoding system parameters in terms of temporal and spatial focusing. For the simulations we consider 10 tap channels with each tap identically and independently distributed (i.i.d) as a circularly symmetric complex Gaussian random variable with mean 0 and variance $\frac{1}{10}$ ¹. The power delay profile is distributed uniformly across the taps for each channel and the expected total channel energy per transmit antenna equals 1. The transmitted signal energy across all antennas is normalized such that total energy transmitted equals 1. The systems simulated with correlated taps have the property

$$\mathbb{E}_h [h_i[\mathbf{r}, m] h_j^*[\mathbf{r}, n]] = \begin{cases} \frac{1}{10} & i = j, m = n \\ \frac{\alpha}{10} & i \neq j, m = n \\ 0 & \text{otherwise} \end{cases}$$

where \mathbb{E}_h denotes mathematical expectation over all possible channel realizations. Additionally, the precoder is designed such that $L = 10$ giving us a fair comparison to time reversal precoding. The plots that follow represent the average performance over all channel realizations.

¹Circularly symmetric complex Gaussian random variables with mean μ and variance σ^2 have the property that the real and imaginary parts are i.i.d. with each value distributed as a Gaussian random variable with mean μ and variance $\frac{\sigma^2}{2}$ [7]

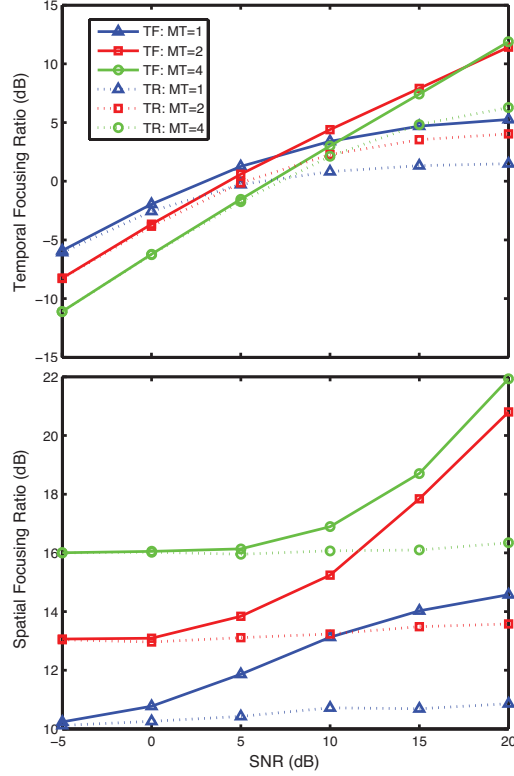


Figure 3: Temporal and spatial focusing ratio for varying number of transmit antennas ($K = 1$)

5.1. Varying M_T

Figure 3 shows the effect of multiple antennas on temporal and spatial focusing with i.i.d. channel entries. For low signal to noise ratios (SNR) $M_T = 1$ yields the best temporal focusing performance. This results from noise dominating at the receiver. Thus, we are no longer concentrating on intersymbol interference cancellation, but maximum energy output in the precoder optimization (i.e. the matched filter or time reversal solution). When multiple transmit antennas are used we spread the energy across antennas (to keep total energy consistent) and (assuming varied channels) reduce total energy received after transmission through the channel. At higher SNR's inter-symbol interference dominates and thus our optimization focuses on interference cancellation. Since multiple antennas allow for more degrees of freedom, our interference cancellation is handled better. Comparing temporal focusing optimal precoders to time reversal precoders we see that (as expected) temporal focusing optimal precoders outperform time-reversal precoders for all SNR values and any number of transmit antennas. It is also interesting to note that the temporal focusing ratio directly relates to the SINR at the receiver. If intersymbol interference is completely cancelled, SNR and SINR are equivalent. A linear trend reflects a constant reduction in the SINR as a

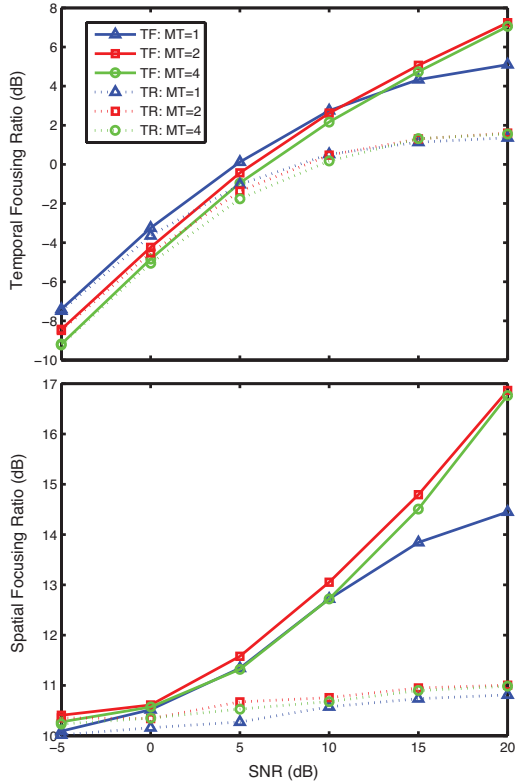


Figure 4: Temporal and spatial focusing ratio for correlated channel ($\alpha^2 = \frac{1}{2}$) varying number of transmit antennas ($K = 1$)

function of SNR. Thus for $M_T = 4$, the SINR is about 7 to 8 dB below the SNR. In other words it takes about 7 to 8 dB to cancel the effects of intersymbol interference.

In terms of spatial focusing, it appears that more antennas imply better performance for virtually all SNR. Spatial focusing relates to how much “different” the channels are between different points in space (since the precoders are functions of the channel). Hence, more transmit antennas allow for more unique effective impulse responses and in turn greater spatial focusing. The results from this plot are very promising. Again, we see that temporal focusing precoders outperform time-reversal precoders in every situation. We also observe that we can obtain from 10 to 20 dB improvement in spatial focusing performance. Since our measure of spatial focusing relates to the ratio of SINR at different points in space, points away from our target have, on average, 10 to 20 dB loss in SINR. This severely inhibits the performance of receivers outside the target. Figure 4 shows the effects of correlation in the frequency selective channels ($\alpha^2 = \frac{1}{2}$). The discussion above for uncorrelated channels still applies, but the gap between the performance due to the number of antennas at the transmitter is narrowed. This makes intuitive sense since the more correlated the channels are, the less diversity available.

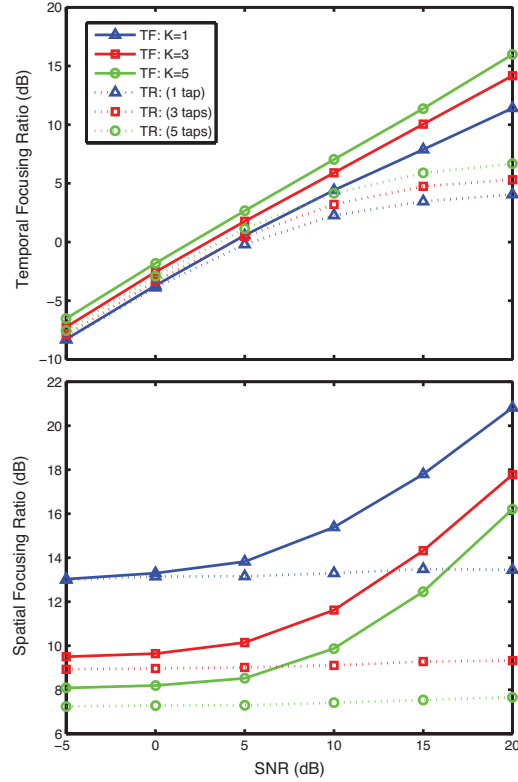


Figure 5: Spatial focusing ratio for varying number of equalizer taps ($M_T = 2$)

5.2. Varying K

We now consider the case where the number of equalized taps in the system response is varied. Figure 5 shows the temporal and spatial focusing performance as a function of SNR for different K values and $M_T = 2$. The temporal focusing ratio is shifted upwards for increasing K . Hence, adding more taps in the equalizer improves the SINR by a constant dB factor. This is an expected result since increasing K relaxes the optimization, allowing us to force more energy into the desired portion of the response. Conversely, increasing K shifts the spatial focusing curves downward as seen in Figure 8. Thus, increasing K decreases the ratio of SINRs at different locations by a constant dB factor. This, is also expected, since as the desired energy lies in a greater portion of the system response, it becomes increasingly more difficult to spatially separate the desired signal energy. Hence, there exists a tradeoff with the K parameter between temporal and spatial focusing.

5.3. Communication System Performance

In this section we preview the performance, in terms of error rate, for time-reversal and temporal focusing optimal precoders. Figure 6 shows a simple bit-error-rate (BER) plot

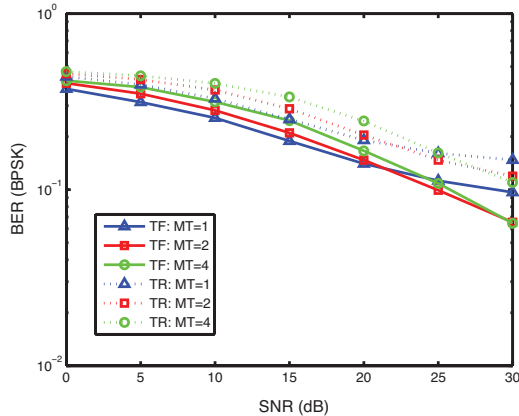


Figure 6: Time reversal, temporal focusing optimal precoder communication system performance comparison ($K=1$)

for time reversal precoders and temporal focusing optimal precoders with varying M_T ($K = 1$). A one-tap equalizer implemented is of minimum mean square error (MMSE) design. Thus, the equalizer is $w_{MMSE} = \frac{d^*[\mathbf{r}, \Delta]}{|d[\mathbf{r}, \Delta] + \sigma^2|}$ (see [11] for details). At first glance, the results may be somewhat unimpressive for both time-reversal precoding and temporal focusing precoding. We must remember, however, that this is for size limited precoders and a one-tap equalizer in a severely frequency selective channel. If we employ longer precoders and more complex equalizers (which all systems with heavy ISI must) we can expect dramatic improvements. This plot is just to compare the temporal focusing precoder and the time reversal precoder in terms of performance. Notice that the temporal focusing precoder outperforms time-reversal for all SNR and all M_T . Additionally, it appears that we only achieve better error rates for multiple antennas in the high SNR regime.

6. CONCLUSION

In this paper we considered a new method of MISO precoding to improve on the benefits of MISO time reversal precoding. By optimizing the precoder in terms of temporal focusing, a property that time reversal precoding exhibits, we were able to outperform time-reversal in terms of temporal focusing, spatial focusing, and error rate performance for nearly all channel situations and system scenarios. This precoding technique offers a feature rarely considered in wireless communications, the ability to spatially focus on receivers. Locations away from the targeted receiver see a dramatically inferior channel. This property may be exploited to increase security in a given communications system.

7. REFERENCES

- [1] M. Fink, "Time reversal of ultrasonic fields - Part 1: Basic principles," *IEEE Trans. Ultrason., Ferroelect., and Freq. Contr.*, Vol. 39, pp. 555-566, Sept. 1992.
- [2] A.J. Paulraj, "Plenary talk: Time reversal in wireless communication," *IEEE Info. Th. Work.*, San Antonio, TX, Dec. 2004.
- [3] P. Melsa, R. Younce, and C. Rohrs, "Impulse response shortening for discrete multitone transceivers," *IEEE Trans. Comm.*, Vol. 44, pp. 1662-1672, Dec. 1996
- [4] C. Oestges, A. Kim, G. Papanicolaou, and A.J. Paulraj, "Characterization of space-time focusing in time-reversed random fields," *IEEE Trans. Ant. and Prop.*, Vol. 53, pp. 283-293, Jan. 2005
- [5] T. Strohmer, M. Emami, J. Hansen, G. Papanicolaou, and A.J. Paulraj, "Application of time-reversal with MMSE equalizer to UWB communications," *Proc. Globecom 2004*, Vol. 5, pp. 3123-3127, Nov. 2004
- [6] B.J. Henty and D.D. Stancil, "Multipath enabled super-resolution for RF/microwave communication using phase-conjugate arrays," *Phys. Rev. Lett.*, Vol. 93, Dec. 2004
- [7] A.J. Paulraj, R. Nabar, and D. Gore, *Introduction to space-time wireless communications*, U.K.: Cambridge Univ. Press, 2003.
- [8] R. Duda, P. Hart, and D. Stork, *Pattern Classification*, Wiley-Interscience, 2000.
- [9] H. Lutkepohl, *Handbook of Matrices*, New York: Wiley & Sons, 1996.
- [10] T.S. Rappaport, *Wireless Communications: Principles and Practice*, Prentice Hall PTR, 2002.
- [11] J. Cioffi, *Digital Communications*, Stanford University Course Reader, 2005.
- [12] G.H. Golub and C.F. Van Loan, *Matrix Computations*, Johns Hopkins University Press, 1996.
- [13] R.F.H. Fischer, *Precoding and Signal Shaping for Digital Transmission*, New York: Wiley & Sons, 2002.
- [14] P. Kyritsi, P. Stoica, G. Papanicolaou, P. Eggers, and A. Oprea, "Time reversal and zero-forcing equalization for fixed wireless access channels," *Conf. Record of the 39-th Asilomar Conf. on Sig., Sys. and Comp.*, pp. 1297 - 1301, 2005.
- [15] M. Schubert and H. Boche, "Solution of the multiuser downlink beamforming problem with individual SINR constraints," *IEEE Trans. Veh. Tech.*, Vol. 53, pp. 18-28, Jan. 2004.